NeuroImage **16,** 1028–1037 (2002)
doi:10.1006/nimg.2002.1145

Neuronal Specificity of Acupuncture Response: A fMRI Study with Electroacupuncture

Ming-Ting Wu,*,† Jer-Ming Sheen,‡ Kai-Hsiang Chuang,§ Pinchen Yang,¶ Shieuh-Lii Chin,‖ Chin-Ying Tsai,* Chung-Jen Chen,** Jan-Ray Liao,†† Ping-Hong Lai,*,† Kuo-An Chu,†,‡‡ Huay-Ben Pan,*,† and Chien-Fang Yang*,†

**Department of Radiology, ‖Department of Rehabilitation, and ‡‡Department of Internal Medicine, Kaohsiung Veterans General Hospital, Kaohsiung 813, Taiwan, Republic of China; †School of Medicine, National Yang Ming University, Taipei, Taiwan, Republic of China; ‡Department of Chinese Medicine, Chang-Chung Memorial Hospital-Kaohsiung Medical Center, Kaohsiung, Taiwan, Republic of China; §College of Electrical Engineering, National Taiwan University, Taipei, Taiwan, Republic of China; ¶Department of Psychiatry and **Department of Internal Medicine, School of Medicine, Kaohsiung Medical University, Kaohsiung, Taiwan, Republic of China; and ††Department of Electrical Engineering, National Chung Hsing University, Taichung, Taiwan, Republic of China*

Received October 5, 2001

Recently, neuronal correlates of acupuncture stimulation in human brain have been investigated by functional neuroimaging. The preliminary findings suggest that acupuncture at analgesic points involves the pain-related neuromatrix and may have acupoint–brain correlation. Although multiple models of control stimulations have been applied to address the specificity of the needling effect clinically, their impacts have not been evaluated by functional neuroimaging. With the advantage of objective parameter setting, electroacupuncture (EA) was used in this study to devise three distinct controls for real EA, i.e., mock EA (no stimulation), minimal EA (superficial and light stimulation), and sham EA (same stimulation as real EA) applied at nonmeridian points. Fifteen healthy volunteers received real EA at analgesic point Gallbladder 34 (Yanglinquan), sham EA, and one of either mock EA or minimal EA over the left leg in counter-balanced orders. Multisubject analysis showed that sham EA and real EA both activated the reported distributed pain neuromatrix. However, real EA elicited significantly higher activation than sham EA over the hypothalamus and primary somatosensory–motor cortex and deactivation over the rostral segment of anterior cingulate cortex. In the comparison of minimal EA versus mock EA, minimal EA elicited significantly higher activation over the medial occipital cortex. Single-subject analysis showed that superior temporal gyrus (encompassing the auditory cortex) and medial occipital cortex (encompassing the visual cortex) frequently respond to minimal EA, sham EA, or real EA. We concluded that the hypothalamus–limbic system was significantly modulated by EA at acupoints rather than at nonmeridian points, while visual and auditory cortical activation was not a specific effect of treatment-relevant acupoints and required further investigation of the underlying neurophysiological mechanisms. © 2002 Elsevier Science (USA)

Key Words: **acupuncture; brain mapping.**

INTRODUCTION

Although the acupuncture of traditional Chinese medicine has gained increasing popularity in modern health care for the past few decades, the scientific basis of acupuncture was not investigated until the 1970s. Among the versatile applications of acupuncture therapy, acupuncture analgesia has the most supporting neurobiological evidence for its effect (Han, 1982; NIH Consensus Conference, 1998). However, the investigation of neuronal correlates of acupuncture in human brain was limited by the lack of a noninvasive method until the recent development of functional brain imaging. With functional magnetic resonance imaging (fMRI) or positron emission tomography (PET), evidence that acupuncture stimulation at analgesic points, such as Large Intestine 4 (LI4) and Stomach 36 (ST36), might modulate the pain-related neuromatrix, i.e., the hypothalamus–limbic system has accumulated (Wu *et al.*, 1997, 1999, Hui *et al.*, 2000; Hsieh *et al.*, 2001; Biella *et al.*, 2001). In addition, a correlation between stimulation at acupoints of proclaimed therapeutic effect for eye disease (Bladder 67, Gallbladder 37 (GB37)) or ear disease (Gallbladder 43 (GB43)) and activation of corresponding brain cortices (visual cortex or auditory cortex, respectively) have been reported (Cho *et al.*, 1998, 2001). These findings suggest that cerebral activation responding to acupuncture stimulation may shed light on the central mechanism of the acupuncture effect.

1053-8119/02 $35.00

Given the fact that acupuncture produces a unique somatosensory reaction, DeQi, it is a methodological challenge to find appropriate controls in conducting single-blinded clinical acupuncture trials (Vincent and Lewith, 1995). It has been proposed that acupuncture induces both specific and nonspecific effects (Vincent *et al.*, 1989; Vincent and Lewith, 1995; Ernst and White, 1997; Lao *et al.*, 2001). To examine acupoint specificity, sham acupuncture was initially devised with needling at nonmeridian points with needle depth, stimulation intensity, and manipulation method identical to those used in real acupuncture (Richardson and Vincent, 1986). However, sham acupuncture has been found to have certain therapeutic effects and cannot be considered a valid placebo. Alternatively, minimal acupuncture (with very light stimulation at superficial nonmeridian points) has been assumed to minimize the therapeutic effect while triggering most of the nonspecific effects of needling (Vincent and Lewith, 1995). In addition, placebo acupuncture (no needle insertion) or mock electroacupuncture (without current applied) have been devised to examine the psychological impact of needling while minimizing both therapeutic and nonspecific effects of needling (Richardson and Vincent, 1986). Although these aforementioned different models of control stimulations have been applied in many clinical acupuncture studies, their impacts on human brain reaction have not been well evaluated by functional brain images in an identical study.

Electroacupuncture (EA) has been developed as an alternative of manual acupuncture, especially in the application of acupuncture analgesia (Han, 1982). It has the advantage of objective settings of stimulation parameters and therefore facilitates development of several distinct models of control stimulation for real EA. In the present study, we used EA at Gallbladder 34 (GB34) (Yanglinquan; an important analgesic acupoint especially for disorders of muscle and tendon) as the study acupoint to test (1) whether EA at an analgesic point (GB34) can activate the pain-related neuromatrix, which may underscore its analgesic mechanism as previously reported by manual acupuncture, and (2) whether the visual and auditory cortex, which have been found to be activated by acupuncture at treatment-relevant GB37 and GB43, respectively (Cho *et al.*, 2001), can be activated also by an analgesic point not relevant to treatment for eye or ear diseases. We also hypothesized that the use of multiple models of control stimulations, i.e., mock EA, minimal EA, and sham EA (Fig. 1 and Table 1), can help address the specificity of neuronal expression of the above issues.

SUBJECTS AND METHODS

Subject Preparation

Fifteen healthy volunteers (age 20–30 years; 10 males, 5 females), all right-handed, were enrolled. All of the subjects had not experienced EA before, and they were given the following instructions before the start of the fMRI experiments. They were informed that different models of EA at various points might be used for comparison. However, the precise locations of needling, the presumed acupuncture effects, and the stimulation paradigm were not divulged. Before the actual fMRI experiments took place, an EA practice session was performed to determine the maximal intensity of EA stimulation that the subject could bear. The practice session was performed on the subject's right leg in a setting similar to that inside an MRI scanner. However, the subjects were not informed what kind of EA was used for the test. During the experiment, the subjects were requested to keep their eyes closed and to use earplugs and headphones to reduce scanner noise. A head stabilization set (Psychology Software Tools, Inc., Pittsburgh, PA) was applied to fix the mandible and adhesive strips were used to fix the forehead and thereby minimize head motion. Informed consent was obtained from each subject. The study was approved by our local Institution Review Board.

Psychophysical Rating of Needling Sensation (DeQi Score)

To evaluate the subjects' response to EA stimulation, self-reported characteristic needling sensation, i.e., DeQi in traditional Chinese medicine, was scored immediately after each session. The DeQi score was simplified as an overall mixture of several sensory perceptions, including numbness, soreness, heaviness, and propagation of the sensations (Beijing College of Traditional Chinese Medicine *et al.*, 1993; Stux and Pomeranz, 1998). A score of 0 denoted no somatosensory sensation at all, 5 denoted the emerging DeQi sensation, and 10 denoted the subject's maximal tolerable DeQi. In cases in which subjects felt pain, notes were made.

Paradigm and Block Design

We applied four models of stimulation, i.e., mock EA, minimal EA, sham EA, and real EA, over the subjects' left legs. The resting states in all four paradigms were characterized by the absence of needling and stimulation. The definitions of the four paradigms are described in detail in Table 1 and the point locations are indicated in Fig. 1 (Beijing College of Traditional Chinese Medicine *et al.*, 1993; Stux and Pomeranz, 1998). One experienced acupuncturist performed all the acupuncture procedures with the use of a dedicated EA device (VGH-82A; Skylark Co., Taiwan, R.O.C.). Another observer who was blinded to the study protocol was assigned to record the needling location and the current (mini-Ampere (mA)) of EA stimulation.

Each experimental session was composed of five blocks lasting 1 min each: Rest–Stimulation–Rest–

TABLE 1

Definition of the Four Types of Electroacupuncture (EA)

	Real EA	Sham EA	Minimal EA	Mock EA	Rest
Subjects	15	15	8	7	15
Location[a]	GB34,[b] lateral area of left leg	4–5 cm from GB34, nonmeridian, lateral area of left leg	4–5 cm from sham point, nonmeridian, lateral area of left leg	= Minimal EA	No needle
Needle depth	2–3 cm	= Real EA	0.3–0.5 cm	= Minimal EA	—
EA, current (mA)	Subjectively optimal	= Real EA	Minimally sensible	—	—
EA, Hz	4	4	4	—	—
Duration	1 min × 2 blocks	1 min × 2 blocks	1 min × 2 blocks	1 min × 2 blocks	1 min × 3 blocks

[a] The locations described here were for one of the paired EA needles. The other needle was placed 1 cm proximally along the gallbladder meridian for real EA or along an imaginary line for the other types of EA.

[b] GB34, Yanglinquan, is located at the point of intersection of the lines from the anterior and inferior borders to the head of the fibula (Stux and Pomeranz, 1998).

Stimulation–Rest. The two stimulation blocks in a given session were of the same model. Each subject participated in three experimental sessions: one session of sham EA ($N = 15$), one session of real EA ($N = 15$), and one of either mock EA ($N = 7$) or minimal EA ($N = 8$). The orders of the three sessions were randomized to be counter balanced. A 15-min interval was interposed between two consecutive sessions.

Magnetic Resonance Imaging

MRI was performed on a 1.5 T MR imager (Signa, GE, Milwaukee, WI) with the following protocols: (1) high-resolution structure images of the whole brain with a T1-weighted three-dimensional (3D) spoiled gradient recall echo sequence; TR = 50 ms, TE = 9 ms, flip angle = 50°, 60 contiguous slices, voxel size = $0.94 \times 0.94 \times 2.9$ mm^3, average = 1; (2) a T1-weighted 2D spin echo axial images parallel to the anterior commissure–posterior commissure line from skull base to vortex; slice thickness = 5 mm, interslice gap = 1 mm, 20 slices, voxel size = $0.94 \times 0.94 \times 5$ mm^3 for structural reference of functional images; and (3) a blood oxygenation level-dependent (BOLD)-contrast functional images; the slice locations were identical to those of the 2D T1WI structure images; TE = 50 ms, flip angle = 90°; voxel size = $3.75 \times 3.75 \times 6$ mm^3, 20 slices, whole brain scan repeated once every 3 s and 100 times in each session.

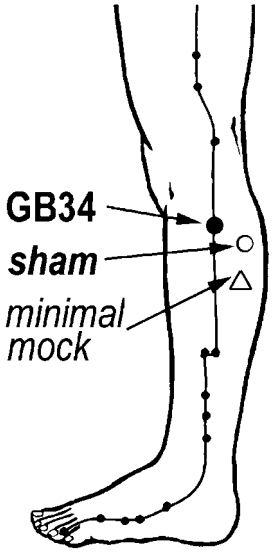

FIG. 1. Illustration of location of the GB34, "Yanglinquan" (solid circle) for real EA and the points for sham EA (empty circle) and minimal EA or mock EA (empty triangle). All are located over the lateral aspect of the left leg.

Image Preprocessing

fMRI data were analyzed using Matlab (Math Works Inc., Natick, MA) and statistical parametric mapping (SPM99; Wellcome Department of Cognitive Neurology, London, UK). The procedure is summarized below; cited references provide fuller mathematical details (Friston *et al.*, 1995; Ashburner and Friston, 1999).

The data were pretreated by removing the first four images to eliminate nonequilibrium effects of magnetization. All volumes of functional images were spatially realigned to the first image to correct for movement using least-squares minimization. A mean image created from the realigned volumes was coregistered with the subject's individual structural T1-weighted volume image. The structural volumes were then spatially normalized to the standard template of the Montreal Neurological Institute (MNI) with nonlinear basis functions (Ashburner and Friston, 1999). The derived spatial transformation was then applied to the realigned BOLD-contrast image volumes with resampling every 3 mm using sinc interpolation, which were finally spatially smoothed with a 9-mm FWHM isotropic Gaussian kernel, to make comparisons between subjects. The resulting time series across each voxel were high-pass filtered with a cutoff of 240 s, using cosine functions to remove section-specific low-fre-

quency drifts in the BOLD signal. The coordinates of activation foci were converted approximately from the MNI coordinates reported using statistical parametric mapping (SPM99) to Talairach coordinates (Talairach and Tournoux, 1988) proposed by Matthew Brett *et al.* (http://www.mrc-cbu.cam.ac.uk/Imaging/mnispace.html).

Statistical Inference

Two levels of statistical inference were used, in accordance with the established SPM conventions discussed in detail elsewhere (Friston *et al.*, 1995; Ashburner and Friston, 1999).

Multisubject analysis. The data were analyzed statistically on a voxel-by-voxel basis using a general linear model with boxcar stimulus functions convolved with a hemodynamic response function to each experimental block. Each contrast produced a statistical parametric map of the *t* statistic for each voxel SPM(*t*), which was subsequently transformed to a unit normal *Z* distribution, SPM(*Z*), for display and tabulation. We used the fixed-effect model because of the known tendency of individuals to respond variably to acupuncture and because we were making inferences about these normal subjects only. The data were thresholded at $P < 0.05$ corrected for multiple comparison (*t* threshold = 4.38) and a spatial extent threshold of 15 voxels. The spatial extent threshold was not applied in the analysis of the hypothalamus, since the target volume is small. The activation foci were superposed on the standard T1 template images.

Single-subject analysis. We used the subject's own brain without spatial normalization to identify the precise activation foci (Fig. 5). To do this, we first coregistered the realigned T2*-weighted BOLD images with the subject's high-resolution T1-weighted volume images, followed by spatial smoothing with a 6-mm FWHM isotropic Gaussian kernel. The data were analyzed statistically on a voxel-by-voxel basis using a general linear model with boxcar stimulus functions convolved with a hemodynamic response function to each experimental block. Each contrast produced a statistical parametric map of the *t* statistic for each voxel SPM(*t*), which was subsequently transformed to a unit normal *Z* distribution, SPM(*Z*), for display and tabulation. The activation survived an uncorrected height threshold of $P < 0.01$, $t = 2.37$ without the spatial extent threshold being reported. The activation foci were superposed on subject's own high-resolution T1-weighted volume images to display the precise location of activation.

RESULTS

DeQi Score and EA Current

The DeQi scores of subjects receiving mock EA (1.52 ± 0.70) were significantly lower than all the others ($P < 0.001$ for all). The DeQi scores of subjects receiving real EA (7.88 ± 1.76) were significantly higher than those of sham EA (5.62 ± 2.05) (Wilcoxon signed ranks test, $P = 0.03$) and those of minimal EA (4.42 ± 2.01) ($P = 0.02$). There was no difference between the scores of subjects receiving sham EA and minimal EA ($P = 0.61$).

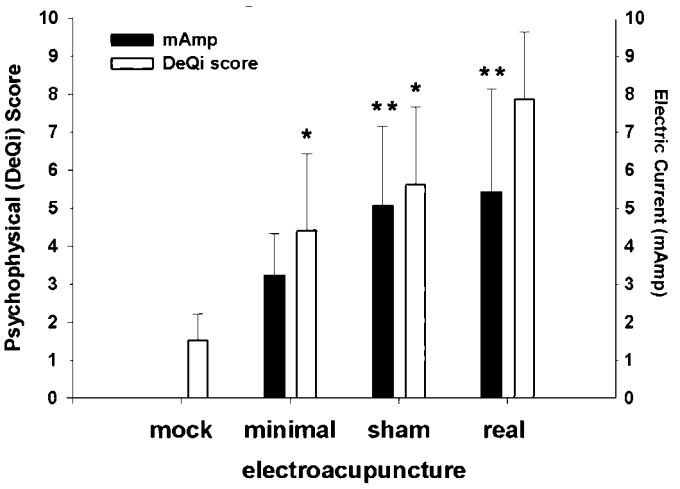

FIG. 2. Bar charts (mean + standard deviation) of psychophysical response of needling sensation (DeQi scores) and electric current (mA, mini-Ampere) in the four models of stimulation. All comparisons were significant ($P < 0.05$) except the pairs labeled with * and **.

With regard to stimulation intensity (electric current) the currents used in real EA (5.41 ± 2.74 mA) and sham EA (5.05 ± 2.11 mA) were not significantly different in paired comparison (Wilcoxon signed ranks test, $P = 0.3$), and both were significantly higher than that used for minimal EA stimulation (3.22 ± 1.12 mA) ($P = 0.01$ for both). No current was applied in mock EA (Fig. 2).

Brain Activation

Multisubject analysis. The results of the multi-subject analysis are summarized in Tables 2 and 3 and Fig. 3. Table 2 lists the results of mock EA and minimal EA compared to resting state and the comparison of minimal EA versus mock EA. Table 3 lists the results of sham EA and real EA compared to resting state and the comparison of real EA versus sham EA. The surface-rendered maps of the activation foci are displayed in Fig. 3. The foci of deactivation (i.e., decreased signal intensity) are shown in Fig. 4.

There were no significant activation foci as a result of mock EA (seven subjects) compared to resting state. In the comparison of minimal EA versus resting state (eight subjects), there was right-side activation of the supplementary motor area, superior temporal gyrus (encompassing the auditory cortex), medial occipital cortex (encompassing the visual cortex), thalamus, and prefrontal and inferior parietal cortices and left-side activation of cerebellum (Fig. 3A).

TABLE 2

Foci of Activation in Multisubject Analysis of Mock EA and Minimal EA

			Mock EA > rest					Minimal EA > rest					Minimal EA > mock EA				
				Talairach's					Talairach's					Talairach's			
Anatomy	Side	BA	Equiv. *Z*	x	y	z	*N*	Equiv. *Z*	x	y	z	*N*	Equiv. *Z*	x	y	z	*N*
Dorsal frontal gyrus	R	6	—	—	—	—	—	7.22	6	−3	63	6	—	—	—	—	—
Superior temporal gyrus (auditory cortex)	R	41/42	—	—	—	—	—	4.76	60	−8	5	3	—	—	—	—	—
Superior temporal gyrus	R	38	—	—	—	—	—	5.71	52	12	−12	4	—	—	—	—	—
Medial occipital cortex (visual cortex)	R	17/18	—	—	—	—	—	>7.84	6	−75	−2	5	6.18	3	−64	19	NA
Thalamus	R		—	—	—	—	—	5.83	6	−14	7	4	—	—	—	—	—
Inferior frontal gyrus	R	44	—	—	—	—	—	7.08	56	12	16	6	—	—	—	—	—
Inferior parietal gyrus	R	40	—	—	—	—	—	6.16	38	−37	42	6	—	—	—	—	—
Cerebellum	L		—	—	—	—	—	6.14	−34	−52	−24	7	—	—	—	—	—
Cerebellum	R		—	—	—	—	—	5.21	52	−42	−28	7	—	—	—	—	—

Note. Height threshold, $t = 4.38$ ($P < 0.05$, corrected for multiple comparison); spatial extent threshold, 15 voxels (for hypothalamus, no extent threshold was used). *N*, number of individuals showing activation at threshold of $t = 2.37$ ($P < 0.01$, uncorrected); extent threshold = 0 voxel. NA, nonapplicable, since minimal EA and mock EA were not performed on same subjects. Talairach's x = right–left, y = anterior–posterior, z = superior–inferior.

In the comparison of minimal EA versus mock EA, there was right-side activation of medial occipital cortex (Fig. 3B).

In the comparison of sham EA versus resting state (15 subjects), there was right-side activation of the primary somatosensory-motor, supplementary motor,

TABLE 3

Foci of Activation in Multisubject Analysis of Sham EA and Real EA

			Sham EA > rest					Real EA > rest					Real EA > sham EA				
				Talairach's					Talairach's					Talairach's			
Anatomy	Side	BA	Equiv. *Z*	x	y	z	*N*	Equiv. *Z*	x	y	z	*N*	Equiv. *Z*	x	y	z	*N*
Postcentral gyrus	R	1/2	>7.84	6	−40	58	13	>7.84	6	−40	58	14	7.38	9	−35	56	12
Postcentral gyrus	R	2	6.77	59	−8	17	10	>7.84	59	−17	19	12	—	—	—	—	—
Postcentral gyrus	L	2	7.80	−57	−20	20	10	>7.84	−54	−17	15	12	—	—	—	—	—
Precentral gyrus	R	4	>7.84	9	−20	64	12	>7.84	9	−20	64	14	6.99	6	−23	59	10
Dorsal frontal gyrus	R	6	>7.84	9	−11	65	12	>7.84	9	−11	65	15	—	—	—	—	—
Superior temporal gyrus (auditory cortex)	R	41/42	6.45	55	−12	10	6	>7.84	56	−12	7	8	—	—	—	—	—
Superior temporal gyrus	R	38	>7.84	54	12	−15	6	>7.84	54	12	−18	8	—	—	—	—	—
Superior temporal gyrus	R	22	6.50	50	0	0	5	>7.84	55	5	−1	7	—	—	—	—	—
Insula	L		—	—	—	—	—	6.6	−41	12	5	8	—	—	—	—	—
Insula	R		—	—	—	—	—	>7.84	45	15	−8	10	—	—	—	—	—
Medial occipital cortex (visual cortex)	R	18	—	—	—	—	—	>7.84	6	−64	−1	6	5.80	9	−67	−1	4
Hypothalamus	R												5.71	3	−3	−8	8
Thalamus	R		>7.84	3	−11	9	9	>7.84	3	−14	15	13	—	—	—	—	—
Anterior cingulate, caudal	R	24/32	—	—	—	—	—	5.88	1	28	35	9	—	—	—	—	—
Anterior cingulate, rostral[a]	R	24/32	4.91	−6	35	−4	8	>7.84	11	39	−5	12	5.94	−4	20	−6	10
Middle frontal gyrus	R	10	—	—	—	—	—	>7.84	−27	59	26	10	5.61	25	62	24	7
Middle frontal gyrus	L	9	—	—	—	—	—	>7.84	−26	56	26	11	—	—	—	—	—
Middle frontal gyrus	L	46	—	—	—	—	—	5.08	40	44	25	7	4.88	−39	35	22	6
Inferior parietal gyrus	R	40	—	—	—	—	—	6.73	38	−55	41	8	—	—	—	—	—
Inferior parietal gyrus	L	40	—	—	—	—	—	6.25	−55	−35	24	8	—	—	—	—	—
Cerebellum	R		>7.84	35	−55	−27	13	>7.84	27	−55	−30	15	—	—	—	—	—
Cerebellum	L		>7.84	−34	−55	−30	14	>7.84	−34	−67	−23	15	—	—	—	—	—

Note. See Table 2 *Note.*

[a] Deactivation (decrease of signal intensity change).

superior temporal gyrus, and thalamus, bilateral activation of secondary somatosensory and cerebellum, and deactivation of rostral segment of anterior cingulate cortex (Figs. 3C and 4). In the comparison of real EA versus resting state (15 subjects), there was right-side activation of the primary somatosensory-motor, supplementary motor, thalamus, caudal segment of anterior cingulate cortex, superior temporal gyrus, and medial occipital cortex and bilateral activation of the secondary somatosensory, insula, prefrontal and inferior parietal cortices, and cerebellum. There was deactivation over the rostral segment of anterior cingulate cortex (Figs. 3D and 4).

In the comparison of real EA versus sham EA (15 subjects), there was right-side activation of the primary somatosensory-motor cortices and medial occipital cortex and bilateral activation of prefrontal cortices. There was activation also over the hypothalamus and deactivation over the rostral segment of anterior cingulated cortex. The thalamus, secondary somatosensory, superior temporal gyrus, insula, and caudal segment of anterior cingulated cortex showed no significant difference (corrected $P > 0.05$) (Figs. 3E and 4).

A tendency of increasing activation over somatosensory-motor cortices, thalamus, anterior cingulate cortex, and insula was noted with increasing EA parameters and DeQi response. In contrast, the activation pattern in the superior temporal gyrus and the medial occipital cortex showed no such tendency (Figs. 2–4).

The activation over two areas deserved further mention. Over the hypothalamus, there was subthreshold deactivation by sham EA ($t = 2.15$) and subthreshold activation by real EA ($t = 3.47$). These subthreshold changes of signal intensity resulted in the significant activation in the comparison of real EA versus sham EA ($t = 5.71$). Similarly, there was subthreshold activation by sham EA over the caudal segment of anterior cingulate cortex ($t = 2.51$); therefore this area showed no significant activation in the comparison of real EA versus sham EA.

Single-subject analysis. The single-subject analysis was focused on the areas showing significant activation/deactivation in the multisubject analysis. The numbers of subjects showing significant activation (uncorrected $P < 0.01$) over those areas are reported in Tables 2 and 3. We confirmed that there were activations over the medial occipital cortex (encompassing the visual cortex, BA 17, 18) and the superior temporal gyrus (encompassing the auditory cortex, BA 41/42) in subjects receiving EA stimulation. However, the activation could be elicited by minimal EA, sham EA, or real EA stimulations. Figure 5 is an example of a subject who showed activation over superior temporal gyrus and medial occipital cortex in response to sham EA (compared to the resting state).

DISCUSSION

In the comparison of real EA at analgesic point GB34 versus resting state, we found several activation areas shared with previously reported areas by manual acupuncture at analgesic acupoints LI4 (Hegu, over dorsal aspect of hand) (Wu *et al.*, 1999; Hui *et al.*, 2000; Hsieh *et al.*, 2001) and ST36 (Zusanli, over medial aspect of leg) (Wu *et al.*, 1999; Biella *et al.*, 2001). These areas, including thalamus, anterior cingulate, insula, and cerebellum, are also part of the reported neuromatrix of pain (Ingvar and Hsieh, 1999; Biella *et al.*, 2001). The consistent pattern of activation elicited by real acupuncture at three different analgesic acupoints from five independent studies, including the present study, supports the notion that acupuncture analgesia may relieve pain by modulating the hypothalamus–limbic system (Wu *et al.*, 1999; Hui *et al.*, 2000; Hsieh *et al.*, 2001; Biella *et al.*, 2001).

With our designations, the difference between sham EA and real EA was limited to the needling point. Accordingly, the comparison of real EA versus sham EA was expected to reveal the acupoint-specific response in the human brain (Lao *et al.*, 2001), which we found to be activation over the primary somatosensory-motor cortex and the hypothalamus and deactivation over the rostral segment of anterior cingulate cortex. In contrast, the activation over caudal segment of anterior cingulate cortex, insula, secondary somatosensory cortex, thalamus, and cerebellum was not significantly related to needling point (Figs. 3 and 4). It should be noted that the sham EA in the present study

FIG. 3. Surface-rendered activation maps on standard structure template by multisubject analysis. (A) Minimal EA compared to rest state (8 subjects). Right-side involvement of supplementary motor area, superior temporal gyrus, medial occipital cortex, thalamus, and prefrontal and inferior parietal cortices and bilateral involvement of cerebellum. (B) Minimal EA (8 subjects) compared to mock EA (7 subjects). Right-side involvement of medial occipital cortex. (C) Sham EA compared to rest state (15 subjects). Right-side involvement of primary somatosensory-motor, supplementary motor, superior temporal gyrus, and thalamus and bilateral involvement of secondary somatosensory cortices and cerebellum. (D) Real EA compared to rest state (15 subjects). Right-side involvement of primary somatosensory-motor, supplementary motor, thalamus, anterior cingulate cortex, superior temporal gyrus, and medial occipital cortex and bilateral involvement of secondary somatosensory, insula, prefrontal, and inferior parietal cortices, and cerebellum. (E) Real EA compared to sham EA (15 subjects). Right-side involvement of medial occipital cortex, primary somatosensory-motor, and hypothalamus and bilateral involvement of prefrontal cortex. No activation foci were noted in superior temporal gyrus. Map of mock EA compared to rest state was not shown since no activation foci survived. The superior temporal gyrus encompasses the auditory cortex and the medial occipital cortex encompasses the visual cortex.

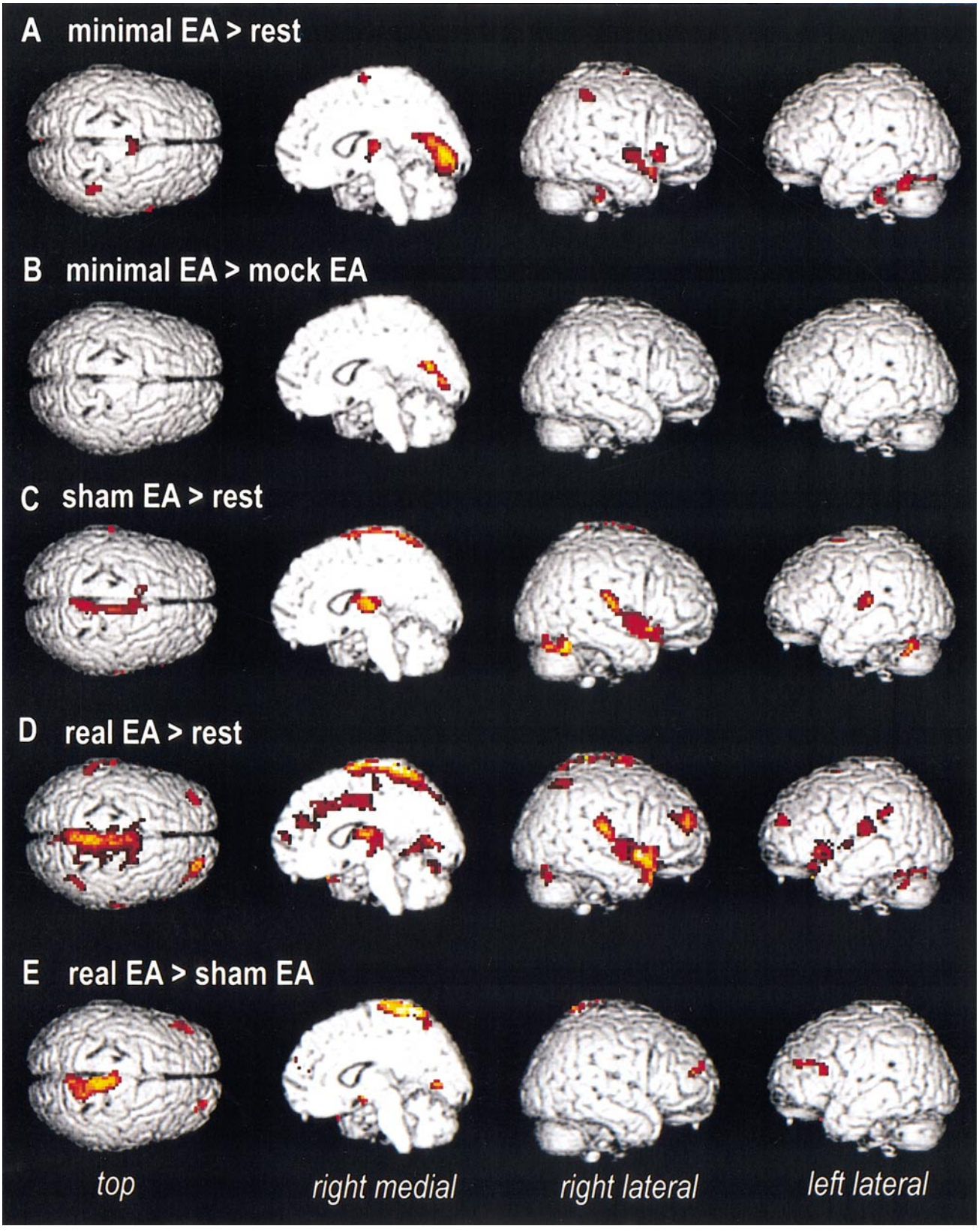
A minimal EA > rest
B minimal EA > mock EA
C sham EA > rest
D real EA > rest
E real EA > sham EA
top
right medial
right lateral
left lateral

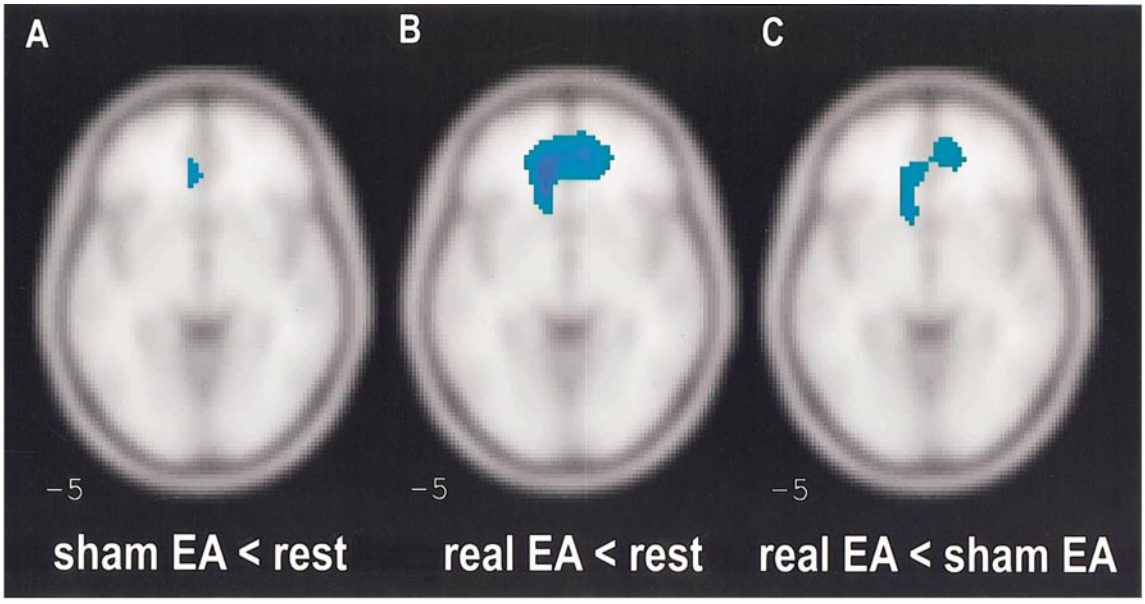

4

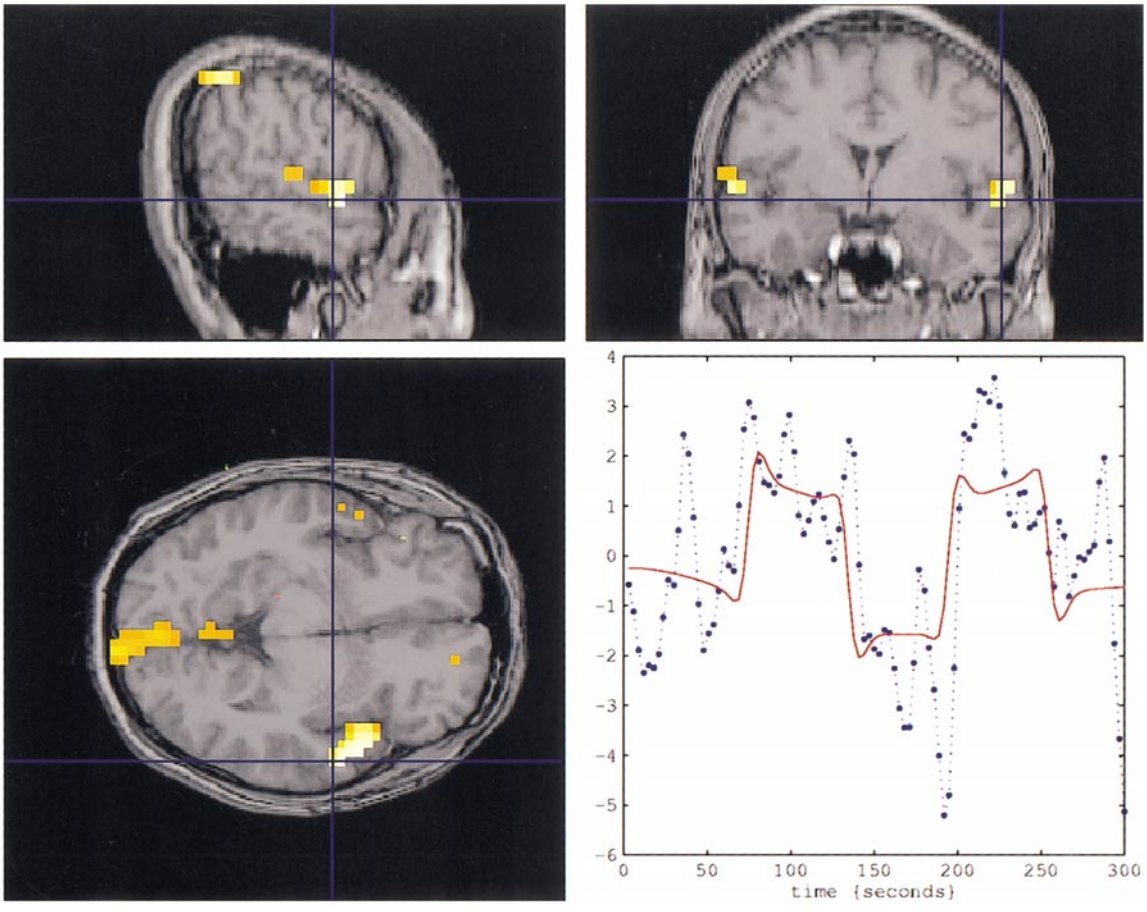

5

FIG. 4. Areas of deactivation in multisubject analysis. The rostral segment of anterior cingulate cortex was the only area showing deactivation. (A) Sham EA minus resting state; (B) real EA minus resting state; (C) real EA minus sham EA.

FIG. 5. Example of a subject showing activation (compared to resting state) of the superior temporal gyrus (encompassing the auditory cortex) and medial occipital cortex (encompassing the vidual cortex) by real EA at acupoint GB34. Three sectional planes were used to locate the foci precisely without spatial normalization. Time course of the signal intensity (right lower) showed a good correlation with the block design of the stimulation.

also elicited DeQi in some cases, which was different from the previous studies using placebo or minimal acupuncture devised to elicit no DeQi at all as controls (Hsieh *et al.,* 2001; Biella *et al.,* 2001). This may explain why there was remarkable overlapping between the activation areas by sham EA and real EA in our findings. Furthermore, we consider the overlapping to support the clinical facts that acupuncture analgesia at sham points works in about 33–50% of patients with chronic pain, while true points work in about 55–85% (Richardson and Vincent, 1986). Nonetheless, the pattern of activation of hypothalamus and deactivation of anterior cingulate cortex by real EA compared to sham EA confirmed our previous proposition that acupuncture at analgesic acupoints activates the pain neuromatrix, i.e., the hypothalamus–limbic system (Wu *et al.,* 1999).

It is interesting to explore whether there is additional evidence of acupoint–brain correlation other than the analgesic aspect of the acupuncture effect. Cho and colleagues (1998, 2001) reported that acupuncture at eye-related acupoints (Gallbladder 37, Bladder 67) and ear-related acupoints (Gallbladder 43) correlated with activation over visual cortex and auditory cortex, respectively. In the present study, with real EA at acupoint GB34 (an important acupoint of the Gallbladder meridian), we also found activation over the medial occipital cortex (encompassing the visual cortex) and superior temporal gyrus (encompassing the auditory cortex). It is interesting to note that GB37, GB43, and GB34 all belong to the Gallbladder meridian and are capable of eliciting activation over the auditory or visual cortex. Future study comparing different meridians may help to define the role of the central pathway of meridians.

However, we found that activation over auditory cortex and visual cortex by EA was not limited to real EA. Sham EA also elicited auditory cortical activation as strong as that by real EA; in addition, minimal EA elicited strong activation over medial occipital cortex relative to that of mock EA (corrected $P < 0.001$). Our findings suggest that acupuncture-induced activation over medial occipital cortex and superior temporal gyrus was not an acupoint-specific phenomenon.

In a study of pain perception, Craig and colleagues (1996) demonstrated visual cortical activation (in their Fig. 1, without discussion) during thermal pain (47°C vs 34°C), but not during warm (40°C vs 34°C) in PET scan. In a study of visceral pain, Baciu and colleagues (1999) reported visual cortical activation (in their Fig. 1 and Table, without discussion) during rectal pain in subjects who kept their eyes closed during fMRI scanning. These examples in nonacupuncture experiments strengthen our proposal that activation over the medial occipital cortex and superior temporal gyrus might be elicited by somatic–visceral sensory stimulation.

Although the underlying neurophysiological mechanism responsible for our findings of medial occipital cortex and superior temporal gyrus activation by minimal EA, sham EA, or real EA is elusive, we suspected that it related to a little-explored sensory cross-modality interaction. This is different from the known interactive inhibition between the visual and the auditory cortices (Kawashima *et al.,* 1995). In addition, the activation over superior temporal gyrus and medial occipital cortex may relate to the complexity of somatotopic projection and the functional organization of thalamocortical relays (Sherman and Guillery, 1996), which means that the activations are in fact not conveying auditory and visual perception per se. This postulation is supported by the fact that our subjects did not experience any visual or auditory perceptions while their medial occipital cortex or superior temporal gyrus showed activation.

It is very interesting and unexpected to find that minimal EA elicited strong medial occipital cortical responses. We speculated that this finding was the result of coincidental (but not intentional) usage of extrameridian nonclassical acupoints in our minimal EA. The existence of extrameridian nonclassical acupoints capable of producing strong therapeutic effect has been noted for long (Beijing College of Traditional Chinese Medicine *et al.,* 1993; Stux and Pomeranz, 1998; Mann, 1998). Since such points are continuously being explored and reported, it might be difficult to avoid them intentionally. In other words, minimal EA at another nonmeridian location may not necessarily produce similar brain activations. It should be also noted that superficial and light stimulation, instead of deep and strong stimulation, has been used as the mainstream in Japanese "shallow" acupuncture (Macdonald *et al.,* 1983; Birch and Ida, 1998). We suggest that further study is required to clarify whether minimal acupuncture can serve as a placebo control (Yamashita and Tsukayama, 2001).

We found there to be individual variation of the cortical activation patterns elicited by EA stimulation (Tables 2 and 3). We think that this finding may underline the clinical observations that there are "nonreactors," "normal reactors," and "strong reactors" of therapeutic response in subjects receiving acupuncture treatment (Beijing College of Traditional Chinese Medicine *et al.,* 1993; Mann, 1998; Stux and Pomeranz, 1998). For this reason, our multisubject analysis was performed with a fixed-effect model, since we were examining the group result from the subjects in this pilot study only.

Finally, while EA has the advantage of objective settings of stimulation parameters, it is certainly possible that EA and manual acupuncture elicit different brain reactions. For example, the primary somatosensory cortex showed strong activation in real EA compared to that in sham EA in the present study, but not

in previous studies using manual acupuncture (Hsieh *et al.*, 2001; Biella *et al.*, 2001). Future study with intrasubject crossover design of manual and electric acupuncture may help to characterize the brain mapping of these two modalities. Nonetheless, we consider both methods appropriate paradigms to explore the central effect of acupuncture.

We conclude that EA is an appropriate method to explore the central effect of acupuncture stimulation, which is enhanced by the use of multiple models of control EA to extract different aspects of acupuncture effect. The hypothalamus–limbic system was significantly modulated by EA at acupoints rather than at nonmeridian points, while visual and auditory cortical activation was not a specific response of treatment-relevant acupoints and requires further investigation of the underlying neurophysiological mechanism.

ACKNOWLEDGMENTS

This work was supported by Grants VGHKS87-45 (Kaohsiung Veterans General Hospital, Taiwan), NSC87-2314-B-075B-002 (National Science Council, Taiwan), and NHRI-GT-EX90-8824EC (National Health Research Institute, Taiwan) to M.-T. Wu. The authors thank the members of the Club of China Traditional Medicine (Kaohsiung Medical University, Taiwan) for their participation and assistance.

REFERENCES

Ashburner, J., and Friston, K. J. 1999. Nonlinear spatial normalization using basis functions. *Hum. Brain Mapp.* **7:** 254–266.

Baciu, M., Bonaz, B., and Segebarth, C. 1999. Central processing of rectal pain: A functional MR imaging study. *Am. J. Neuroradiol.* **20:** 1920–1924.

Beijing College of Traditional Chinese Medicine, Shanghai College of Traditional Chinese Medicine, Nanjing College of Traditional Chinese Medicine, and The Acupuncture Institute of the Academy of Traditional Chinese Medicine. 1993. *Essentials of Chinese Acupuncture.* Foreign Language Press, Beijing.

Biella, G., Sotgiu, M. L., Pellegata, G., Paulesu, E., Castiglioni, I., and Fazio, F. 2001. Acupuncture produces central activations in pain regions. *NeuroImage* **14:** 60–66.

Birch, S., and Ida, J. 1997. A brief report on the 1996 U.S. Toyohari workshop, with reflections on the development of Keiraku chiryo (Japanese meridian therapy) in America. *Amer. J. Acu.* **25:** 71–74.

Cho, Z.-H., Chung, S.-C., Jones, J. P., Park, J. B., Park, H. J., Lee, H.-J., Wong, E. K., and Min, B.-I. 1998. New findings of the correlation between acupoints and corresponding brain cortices using functional MRI. *Proc. Natl. Acad. Sci. USA* **95:** 2670–2673.

Cho, Z.-H., Na, C.-S., Wang, E. K., Lee, S.-H., and Hong, I.-K. 2001. Functional magnetic resonance imaging of the brain in the investigation of acupuncture. In *Clinical Acupuncture—Scientific Basis* (G. Stux and R. Hammerschlag, Eds.), pp. 83–96. Springer-Verlag, Berlin.

Craig, A., Reiman, E., Evans, A., and Bushnell, M. 1996. Functional imaging of an illusion of pain. *Nature* **384:** 258–260.

Ernst, E., and White, A. R. 1997. A review of problems in clinical acupuncture research. *Am. J. Clin. Med.* **25:** 3–11.

Friston, K. J., Holmes, A. P., Woresley, K., Poline, J. B., Frith, C., and Frackowiak, R. S. J. 1995. Statistical parametric maps in functional imaging: A general linear approach. *Hum Brain Mapp.* **2:** 189–210.

Han, J.-S. 1982. Neurochemical basis of acupuncture. *Annu. Rev. Pharmacol. Toxicol.* **22:** 193–220.

Hsieh, J., Tu, C., Chen, F., Chen, M., Yeh, T., Cheng, H., Wu, Y., Liu, R., and Ho, L. 2001. Activation of the hypothalamus characterizes the acupuncture stimulation at the analgesic point in humans: A positron emission tomography study. *Neurosci. Lett.* **307:** 105–108.

Hui, K. K., Liu, J., Makris, N., Gollub, R. L., Chen, A. J., Moore, C. I., Kennedy, D. N., Rosen, B. R., and Kwong, K. K. 2000. Acupuncture modulates the limbic system and subcortical gray structures of the human brain: Evidence from fMRI studies in normal subjects. *Hum. Brain Mapp.* **9:** 13–25.

Ingvar, M., and Hsieh, J. 1999. The image of pain. In *Textbook of Pain* (P. D. Wall and R. Melazck, Eds.), pp. 215–234. Churchill, London.

Kawashima, R., O'Sullivan, B. T., and Roland, P. E. 1995. Positron-emission tomography studies of cross-modality inhibition in selective attentional tasks: Closing the "mind's eye." *Proc. Natl. Acad. Sci. USA* **92:** 5969–5972.

Lao, L., Ezzo, J., and Berman, B. M. H. R. 2001. Assessing clinical efficacy of acupuncture: Considerations for designing future acupuncture trials. In *Clinical Acupuncture—Scientific Basis* (G. Stux and R. Hammerschlag, Eds.), pp. 187–209. Springer-Verlag, Berlin.

Macdonald, A. J., Macrae, K. D., Master, B. R., and Rubin, A. P. 1983. Superficial acupuncture in the relief of chronic low back pain. *Ann. R. Coll. Surg. Engl.* **65:** 44–46.

Mann, F. 1998. A new system of acupuncture. In *Medical Acupuncture* (J. Filshie and A. White, Eds.), pp. 61–66. Churchill, Edinburgh.

NIH Consensus Conference. 1998. Acupuncture. *J. Am. Med. Assoc.* **280:** 1518–1524.

Richardson, P. H., and Vincent, C. A. 1986. Acupuncture for the treatment of pain: A review of evaluative research. *Pain* **24:** 15–40.

Sherman, S. M., and Guillery, R. W. 1996. Functional organization of thalamocortical relays. *J. Neurophysiol.* **76:** 1367–1395.

Stux, G., and Pomeranz, B. 1998. *Basics of Acupuncture,* 4th ed. Springer-Verlag, Berlin.

Talairach, J., and Tournoux, P. 1988. *Co-Planar Stereotaxic Atlas of the Human Brain.* Thieme, New York.

Vincent, C. A., Richardson, P. H., Black, J. J., and Pither, C. E. 1989. The significance of needle placement site in acupuncture. *J. Psychosom. Res.* **33:** 489–496.

Vincent, C., and Lewith, G. 1995. Placebo controls for acupuncture studies. *J. R. Soc. Med.* **88:** 199–202.

Wu, M.-T., Xiong, J., Yang, P.-C., Hsieh, J.-C., Tsai, G., Rosen, B. R., and Kwong, K. K. 1997. Acupuncture modulating the limbic brain detected by functional MR imaging. *NeuroImage* **5:** S15.

Wu, M.-T., Hsieh, J.-C., Xiong, J., Yang, C.-F., Pan, H.-B., Chen, Y.-C., Tsai, G., Rosen, B. R., and Kwong, K. K. 1999. Central nervous pathway for acupuncture stimulation: Localization of processing with functional MR imaging of the brain—Preliminary experience. *Radiology* **212:** 133–141.

Yamashita, H., and Tsukayama, H. 2001. Minimal acupuncture may not always minimize specific effects of needling. *Clin. J. Pain* **17:** 277.